

# Equilibrium and Thermodynamic Studies of Reactive Orange Dye Biosorption by Garden Grass

**Ahmed A. Mohammed**  
Assistant Professor  
College of Engineering  
University of Baghdad  
ahmed.abedm@yahoo.com

**Farrah Emad Al-Damluji**  
Assistant Lecturer  
College of Engineering  
University of Baghdad  
farrah.damluji@yahoo.com

**Tariq J. Al-Musawi**  
Lecturer  
College of Engineering  
University of Baghdad  
tariqjad@yahoo.com

## ABSTRACT

The present study aims to evaluate the biosorption of reactive orange dye by using garden grass. Experiments were carried out in a batch reactor to obtain equilibrium and thermodynamic data. Experimental parameters affecting the biosorption process such as pH, shaking time, initial dye concentrations, and temperature were thoroughly examined. The optimum pH for removal was found to be 4. Fourier transform infrared spectroscopy analysis indicated that the electronegative groups on the surface of garden grass were the major groups responsible for the biosorption process. Four sorption isotherm models were employed to analyze the experimental data of which Temkin and Pyzhey model was found to be most suitable one. The maximum biosorption capacity was 12.2 mg/g at 30 °C. The maximum removal percent reached 90% at optimum conditions. Therefore, the pretreatment or modification of this biosorbent may enhance the biosorption capacity. Thermodynamic parameters (i.e., change in the free energy, the enthalpy, and the entropy) were also evaluated and their values revealed that the biosorption process was exothermic in nature and less favorable at high temperature.

**Keywords:** grass, orange dye, biosorption, isotherm model, thermodynamic.

## دراسة توازن وثرموداينمكية الامتزاز الحيوي للصبغة البرتقالية باستخدام ثيل الحدائق

طارق جواد الموسوي  
مدرس  
جامعة بغداد/كلية الهندسة

فرح عماد الدملوجي  
مدرس مساعد  
جامعة بغداد/كلية الهندسة

احمد عبد محمد  
استاذ مساعد  
جامعة بغداد/كلية الهندسة

## الخلاصة

تهدف الدراسة الحالية الى تقييم الامتزاز الحيوي للصبغة البرتقالية الفعالة باستخدام ثيل الحدائق. اجريت العديد من التجارب بطريقة الدفعات لغرض الحصول على بيانات الامتزاز الحيوي و الثرموداينمكية. تم دراسة تأثير بعض الظروف في عملية الامتزاز مثل الدالة الحامضية، سرعة الخلط، التركيز الابتدائي، والحرارة. وجد ان افضل ازالة حصلت عند قيمة دالة الحامضية 4. بينت نتائج تحليل الثيل باستخدام الاشعة تحت الحمراء (FTIR) ان المجاميع الفعالة سالبة الشحنة الموجودة على سطح الثيل كان لها الدور الكبير في عملية الامتزاز. تم مطابقة النتائج العملية مع اربعة موديلات رياضية حيث بينت النتائج تطابق كبير مع الموديل المقدم من قبل Temkin و Pyzhey. وصلت اعلى قيمة لعملية الامتزاز الى 12.2 ملغم/غم عند درجة حرارة 30 مئوية. و ان اعلى نسبة ازالة وصلت الى 90% بالظروف المثلى. لذا فان عملية المعالجة او التعديل للمادة الممتزة

ربما تحسن عملية الازالة. اثبتت نتائج دراسة الثرموداينمك ان طبيعة الامتزاز هو باعث للحرارة و غير مفضل بدرجات الحرارة العالية.

**كلمات رئيسية:** ثيل، صبغة برتقالية، امتزاز الحيوي، موديل، ثرموداينمك.

## 1. INTRODUCTION

Reactive dyes are extensively used in textile, paper, leather, plastic, cosmetics, pharmaceuticals, and food industries to color various substances, **Han, and Yun, 2007**. These dyes are widely used to dye cotton, wool, and polyamide fibers, due to their properties such as simple application procedure, good stability during washing, and bright colours. Dyes are bright in color due to presence of one or several azo bonds (-N=N-) associated with substituted aromatic structures, **Moreira, et al., 1998; Bhatnagar, and Jain, 2005**. Wastewaters from textile industry contain large amounts of dyes, representing a major threat to the environment due to their toxicity and potential carcinogenic nature, **Bizani, et al., 2006**. Dyes are the most easily recognized contaminant because they are visible to the human eye. Dyestuff effluent is resistant to light and when discharged into the water bodies, it prevents the sunlight from penetrating through and reduces the aesthetic quality of water and photosynthesis, **Owoyokun, 2009 and Jiang, et al., 2008**). Therefore, it is necessary for the dye effluents to be treated properly before they are discharged into the water bodies. A number of conventional treatment methods like coagulation, chemical precipitation, membrane filtration, solvent extraction, chemical oxidation, photolysis, reverse osmosis, and flocculation have been used for the treatment of dyes containing wastewaters, **Mittal, et al., 2009**. However, these methods are generally ineffective in color removal and expensive for the treatment of dyes containing wastewaters due to their complex poly-aromatic structure and hence cause health problems, **Mahmoud, et al., 2007 and Mall, et al., 2007**.

Adsorption techniques are generally considered as the preferred means for removing dyes due to their efficacy to separate chemical compounds from wastewater, simple operation, easy recovery and reuse of adsorbent. The most widely used adsorbent for this purpose is activated carbon, **El-Sayed, et al., 2011**, however, due to economic constraint, its applications on industrial scale are limited, **Hammed, et al., 2008**. Biosorption is a process which utilizes inexpensive dead biomass to remove pollutants from waters, especially those that not easily degradable such as metals and dyes, **Kratochvil, and Volesky, 1998**. Biosorption is proven to be quite effective at removing pollutants from contaminated solutions in a low cost and environment-friendly manner, **Sulaymon, et al., 2013**. Biosorption of dyes from wastewater has attracted a significant attention in recent years. A number of studies have been focused on biomaterials that are capable of removing dyes from wastewater such as deoiled soya, **Mittal, et al., 2009**, barely husk, **Haq, et al., 2011**; sunflower, **Thinakaran, et al., 2007**; rice milling waste, and **Bhatti, and Safa, 2012**, etc. However, these biosorbents have generally low biosorption capacities, high cost, not available in high quantity. Therefore, there is a need to find new, economically, easily available and effective biosorbent. Grass is an agricultural waste, environmentally friendly, and high yield material after mowing gardens, lawns, and parks. Grass is available in large quantities in gardens in University of Baghdad. Approximately, ten tons of grass is mowed monthly from these gardens. Often, these quantities were dumped in a municipal solid waste landfill. In addition, GG is a low cost biosorbent, the unit cost of collecting 1 kg of virgin grass from Baghdad University gardens is about US\$ 0.5, **Sulaymon, et al., 2014**. Several studies have been carried out to examine the use of grass as biosorbent to remove heavy metals from aqueous solution. **Hossain,**

et al., 2012, Sulaymon, et al., 2014, and Chojnacka, 2006, studied the heavy metal removal efficiency of grass. The results revealed that the garden grass was an effective biosorbent for the removal of heavy metals.

In this study, we focused on the removal of reactive orange (RO) dye from aqueous solution onto garden grass (GG). The preparation, characterization and sorption properties of GG were reported. RO dye sorption was investigated in batch system considering the effect of pH, temperature, contact time, and initial dye concentration.

## 2. MATERIALS AND METHODS

### 2.1. Biosorbent and Sorbate Preparation

The GG was collected from the gardens of University of Baghdad after mowing. The foreign matters were removed manually. To remove dirt and impurities, the GG washed several times with tap water then with distilled water. Cleaned GG was cut into small pieces, sundried, and then dried in oven at  $60 \pm 3$  °C until all the moistures are removed. The dried material was shredded, grounded into powder. The average particle size of powdered grass was measured by sieving method in a sieve shaker. The average size of GG particles that passed the 200  $\mu\text{m}$  size screen (yield 50 %) were chosen as biosorbent then stored in an opaque air-tight polyethylene container at room temperature for using in the biosorption experiments with required amounts. No other physical or chemical treatment was used before biosorption experiments.

The commercial grade of RO dye with molecular formula  $\text{C}_{20}\text{H}_{17}\text{N}_3\text{Na}_2\text{O}_{11}\text{S}_3$ , molecular weight 617.42 g/mol, and wave length ( $\lambda_{\text{max}}$ ) 490 nm, solubility 90 mg/l, pH 6.5, was obtained from SIGMA-ALDRICH Company. **Fig. 1** shows the chemical structure of RO dye used in this study. Simulated stock solution of RO dye had been prepared by dissolving 1 g of dry powdered dye in 1000 ml distilled water and stored in glass container at the room temperature. Experimental solutions of desired concentrations ranging from 10 to 100 mg/l were obtained by successive dilution of the stock solution. The initial pH of the working solutions was adjusted by addition drop-by-drop buffer solution under magnetic stirring. Standard curve were developed at  $\lambda_{\text{max}}$  490 nm for RO dye through the measurement of the dye solution absorbance by UV-VIS spectrophotometer (Model: APEL PD-303 UV, JAPAN). All the glassware used for dilution, storage and experimentation were cleaned with detergent, thoroughly rinsed with tap water, soaked overnight in a 20%  $\text{HNO}_3$  solution and finally rinsed with distilled water before use.

### 2.2. Fourier Transfer Infrared Spectroscopy (FTIR) Analysis

The identification of functional groups on the surface of the GG was performed using Fourier transform infrared spectroscopy (FTIR) analysis. The FTIR offers excellent information on the nature of the bands present on the surface of the biosorbent and also presents three main advantages as an analytical technique: it is fast, nondestructive and requires only small sample quantities, **Pereira, et al., 2003**. Two samples of well powdered and dried GG were subjected to the FTIR analysis. The first sample contains 1 g of GG. The second sample was prepared by mixing 1 g of GG with 100 ml of 10 mg/l RO dye solution. The suspension was shaken at 200 rpm for 2 h using a shaker (Edmund Buhler, 7400 Tubingen Shaker-SM 25, Germany). The aqueous solution was withdrawn and then the residue was filtered and dried in oven at 50 °C for 24 h. The two samples were pressed into small discs by using a spectropically pure KBr matrix.

Then, Spectra were registered from 4000 to 500  $\text{cm}^{-1}$  using Fourier transform infrared spectroscopy (Model: SHIMADZU 8500S, Japan).

## 2.3. Batch Experiments

### 2.3.1. Effects studies

Optimization of various parameters such as pH, temperature, initial dye concentration, and shaking time on the removal efficiency were carried out in a batch reactor using classical approach. To study the effect of pH, several conical flasks were shaken at 200 rpm for 4 h. Each flask containing 1 g GG with 100 ml of 10 mg/l dye concentration at room temperature, and the pH range was from 2-8. The temperature effect experiment was conducted using seven flasks each one containing 100 ml of 10 mg/l dye concentration, and the solution temperatures were 20, 25, 30, 35, 40, 45, and 50°C (200 rpm for 2 h, at an optimum pH determined in the pH study). The temperature was maintained using shaker incubator. Effect of initial dye concentrations were conducted using 10, 20, 50 and 100 mg/l dye solutions at room temperature and optimum pH value. The effect of contact time on the sorption process was investigated at different GG dosages (1, 2, 5, and 10 g) with 100 ml of 10 mg/l dye solution. The system was subjected to an agitation speed of 200 rpm, and the samples were collected from 1 to 240 min to determine the remaining concentration of RO dye.

### 2.3.2. Equilibrium experiments

Equilibrium sorption isotherms are useful to understand the sorption interaction as well as to find the sorption capacity of the sorbent. Equilibrium experiments were carried out by agitation fixed amount of GG (0.2, 0.4, 0.6, 0.8, 1, 2, 3, 4, and 5 g) with 100 ml of 10 mg/l synthetic solution of RO dye at different temperature (10, 20, and 30 °C). The pH of solution was adjusted to the best value based on the pH study (i.e., 4). The flasks were placed in a shaker (Edmund Buhler, 7400 Tubingen Shaker-SM 25) with constant shaking speed at 200 rpm for 2 h. After the equilibrium time of biosorption process, the sorbent was separated from the aqueous solution by using a filter paper (WHATMAN, No.42; diameter, 7 cm) and determination of RO dye concentration was conducted by using UV-VIS spectrophotometer. Each sample was measured thrice in UV-VIS spectrophotometer and the results were given as the average value. The dye uptake and the percentage removal were calculated using the following equations:

$$q_e = \frac{(C_o - C_e)V}{m}, \text{ Hossain, et al., 2012} \quad (1)$$

where,  $q_e$  is the equilibrium biosorption capacity (mg/g);  $C_o$  and  $C_e$  are the initial and equilibrium dye concentrations in the water (mg/l), respectively;  $V$  is the volume of used solution (l); and  $m$  is the mass of the used GG.

The percentage of RO dye removal (%) was calculated using the following equation:

$$\% \text{ Removal} = \frac{C_o - C_e}{C_o} \times 100 \quad (2)$$

## 2.4. Methods

The sorption isotherm data can be modeled using a huge number of theoretical equations. In this study, the experimental isotherm data were fitted with the four isotherm models, namely, Langmuir, Freundlich, Redlich-Peterson, and Temkin and Pyszhey sorption isotherm models to describe the equilibrium characteristics of sorption. These models are presented in **Table 1**. Langmuir model assumes monolayer coverage of adsorbate over a homogeneous adsorbent surface, **Langmuir, 1918**. A basic assumption is that sorption takes place at specific homogeneous sites within the adsorbent. The Freundlich isotherm can be applied to non-ideal

adsorption on heterogeneous surfaces as well as multilayer sorption, **Freundlich, 1906**. Temkin and Pyzhey isotherm contains a factor that explicitly taking into the account of sorbent–sorbate interactions. By ignoring the extremely low and large value of concentrations, the model assumes that heat of sorption of all molecules in the layer would decrease linearly rather than logarithmic with coverage, as implied in the Freundlich equation, **Temkin and Pyzhey, 1940**. The Redlich-Peterson isotherm model can be applied to expresses the sorption process when dealing with a certain pollutants at high concentration, **Quintelas, et al., 2008**. In addition, the thermodynamics parameters of the sorption process such as enthalpy changes ( $\Delta H^\circ$ ), entropy changes ( $\Delta S^\circ$ ), and Gibbs free energy changes ( $\Delta G^\circ$ ) were used to determine the spontaneity of biosorption process. These parameters have been determined using Van't Hoff and Gibbs free energy equations.

### 3. RESULTS AND DISCUSSION

#### 3.1. Biosorbent Characterization

The Physicochemical properties of GG are presented in **Table 2**. The FTIR spectrum of GG **Fig.2** shows RO dye interaction with different chemical groups during the biosorption process. This figure shows that the hydroxyl (-OH), carboxyl (-COO), alcohol (C-O), sulfur groups such as C-S-O and S=O stretching and amide groups are involved in the biosorption process. After contact with RO dye solutions, the position of the band related to the -OH groups from cellulose materials and -NH groups from proteins, **Prasad and Santhi, 2012** and **Bertagnolli, et al., 2014**, shifts from  $3338\text{ cm}^{-1}$  in the GG to  $3303\text{ cm}^{-1}$  for RO dye loaded GG. The band observed at  $2911\text{ cm}^{-1}$  is assigned for the alkyl chains (-C-H), **Ahmad, and Kumar, 2010**. This band was slightly shifted to a new value of  $2920\text{ cm}^{-1}$ . The band at  $1641\text{ cm}^{-1}$  could be owing to the presence of carboxylates (-COO) groups, **Arief, et al., 2008**, this group shifted to  $1655\text{ cm}^{-1}$  after RO sorption. The -C-O, C-C, and -C-OH stretching vibrations can be attributed to peaks in the region of  $1440\text{--}1024\text{ cm}^{-1}$ . Some bands in the fingerprint regions ( $900\text{--}750\text{ cm}^{-1}$ ) could be attributed to the aromatic (-C-H) groups, **Al-Rub, et al., 2006**. No change was obvious in these peaks values. The shift of the bands can probably be attributed to proton exchange occurring during the biosorption of the RO dye onto the GG.

#### 3.2 Effect of pH

**Fig.3** shows the results of pH effect study. It can be seen that the pH of solution played a significant role in the sorption process especially in the acidic values. It is noteworthy that varied removal efficiency values were observed in the pH range from 2 to 6. The removal efficiency increased with increasing pH from 2 to 4 and reached to the maximum value (58%) at pH 4. While it reached 90% at the same pH value with using 10g GG. This pattern of dye removal is characteristic of anion sorption. In the pH range 6-7 a small decrease in the removal efficiency is observed while the variation in removal efficiency remain negligible in the pH above 7. **Lodeiro, et al., 2004** showed at high acidic solution, the active surface sites of the sorbent may dissociated, reducing the number of binding sites for the sorption of sorbate. Hence low sorption capacity was observed at pH below 3. At pH range from 3 to 5, the surface of GG becomes positively charged and this facilities sorption of RO dye leading to maximum removal efficiency at pH 4. The results obtained in this study are in a good agreement with those reported in previous studies, **Elwakeel, et al., 2014**, who noted that in acidic solutions more protons will be available to protonate amine groups to form  $-\text{NH}_3^+$  groups, leading to increase of available sorption sites on the adsorbent. A decline in the sorption capacity was observed at pH above 6, which may be attributed to the competition of  $\text{OH}^-$  and dye anions. Also, certain chemical compounds in RO dye such as phenols and acids that are proton donors become anions when the

solution pH reaches to the equilibrium condition, in this case the sorption capacity decreased with increase in pH, **Kookana, and Rogers, 1995**. Therefore, the optimum pH 4 was used for the subsequent experiments.

### 3.2 Effect of Temperature

The effect of temperature on the removal efficiency has been investigated within a temperature range of 20 to 50 °C and the results are depicted in **Fig. 4**. It can be seen that the maximum percentage removal for RO dyes observed between 20-30 °C. Several authors showed that further increases in temperature (above 30 °C) lead to a decrease the percentage removal. This may be attributed to an increase in the relative desorption of the dye from the solid phase to the liquid phase, deactivation of the biosorbent surface, destruction of active sites on the biosorbent surface due to bond disruption, **Saleem, et al., 2007** and **Meena, et al., 2005**, or due to the weakness of the sorbent active site binding forces and the sorbate species and also between the adjacent molecules of the sorbed phase, **Sari, and Tuzen, 2008**. It can be seen from **Fig. 4** that the variation of temperature from 25 to 30 °C has minimal effect on the biosorption process, so that further experiments were carried out at room temperature without temperature adjustment.

### 3.3 Effect of Initial Dye Concentration

**Fig. 5** shows the variation of the removal efficiency and uptake with the variation of initial RO dye concentration from 10 to 100 mg/l at 1 g of GG. The results indicated that the percentage removal was not altered greatly from concentrations between 10 to 20 mg/l, this may be due to the amount of GG used in this experiment contains enough sorption surfaces and sites for this concentration range, **Anwar, 2010**, thereafter the percentage removal rapidly decreased with the further increase in concentration to 20 mg/l. The decrease in the percentage removal of dye can be explained with the fact that all the sorbents had a limited number of active sites, which have become saturated above a certain concentration, **Li, et al., 2012**.

### 3.4 Effect of Contact Time and Dose

It was very important to know the required time to reach equilibrium sorption condition. **Fig. 6** shows the results of sorption efficiency versus contact time. The results revealed a rapid sorption of RO dye at the initial time (30 min). The equilibrium condition was attained within first hour contact time and a relatively slow phase was observed beyond this time period. Initial biosorption was rapid due to the sorption of dye onto exterior surface, after that dye molecules enter into pores (interior surface), relatively slow process. The figure also showed that the removal efficiency increased from (58%-90%) with increasing the GG dosage from (1g to 10g). A similar observation was previously reported from removal of hazardous cationic dyes from aqueous solution onto *Acacia nilotica* leaves, **Prasad, and Santhi, 2012**.

### 3.5 Equilibrium Isotherm Study

The biosorption isotherm is a plot that shows the equilibrium uptake ( $q_e$ , mg/g) against the weight of the biosorbent (g) or equilibrium concentration of the solute in the solution  $C_e$  (mg/g), **Radnia, et al., 2012**. In this study, this was obtained by the measurement of equilibrium uptake of RO dye using GG doses range from 0 to 5 g at different temperature (10, 20, and 30 °C) and the results are depicted in **Fig.7**. The sorption isotherm showed a steep initial slope followed by a progressive saturation of the sorbent. From **Fig.7** it can be seen that the values of biosorption capacity increased with the increase of the GG dose in the range from 0 to 3 g, and then the biosorption capacity reached a plateau. The static biosorption capacity (12.2 mg/g) of the GG sorbent for RO dye was obtained at 30 °C. The experimental isotherm data were fitted with

several equilibrium isotherm models. **Table 3** summarized the parameters of each model; these parameters are obtained from the nonlinear regression using STATISTICA program. The Temkin and Pyzhey model gave the best fit for the experimental data for sorption system of RO dye onto GG compared with other models recognized by the highest coefficient of regression values ( $R^2$ ). The best fit of experimental data by Temkin and Pyzhey isotherm assumes that the fall in the heat of sorption is linear rather than logarithmic, **Temkin, and Pyzhey, 1940**. In addition, the positive values of B of Temkin and Pyzhey model indicated that the biosorption process is a physical process, **Dada, et al., 2012**.

Several efforts have been made to characterize the organic materials binding properties of various forms of biomass. The uptake value by different biomass is summarized in **Table 4**. It can be seen that the GG has a low biosorption capacity, when compared with other biomass, which may be owing to the fact that these biosorbents were treated or modified before using it in the biosorption process.

### 3.6 Thermodynamics Study

Van't Hoff equation is used to obtain the thermodynamics parameters. The values of  $\Delta H^\circ$  (-43.521 kJ/mol) and  $\Delta S^\circ$  (-0.152 J/mol.K) are reported together with the Gibbs free energy values in **Table 5**. The negative value of  $\Delta H^\circ$  indicates the exothermic nature of biosorption process. The values of enthalpy are coherent with chemical nature of the interaction, which confirms the formation of a complex between GG active sites and RO dye. These results are in agreement with the **Elwakeel, et al., 2004**. The negative value of  $\Delta S^\circ$  means a decrease of the randomness of the system during biosorption of RO dye. Gibbs free energy of biosorption was calculated from the eq. (8) mentioned in **Table 1** and the results were listed in **Table 5**. The positive values of  $\Delta G^\circ$  indicate that the biosorption reaction becomes less favorable at high temperature. The increase in the values of  $\Delta G^\circ$  with increasing temperature (from 1.28 to 6.1 kJ/mol) may be attributed to the exothermic nature of the reaction between GG sites and RO dye molecules.

## 4. CONCLUSIONS

This study entailed the equilibrium and thermodynamic studies of the biosorption of RO dye on GG. The results showed that garden grass is a good biosorbent towards reactive orange dye at slightly acidic solution (i.e., optimum pH 4) in which the removal efficiency reached to 90%. The maximum equilibrium uptake was 12.7 mg/g at the optimum condition. The biosorption process was examined by changing various parameters such as pH, temperature, and initial dye concentration, the results showed that the removal efficiency was affected due to the change in these parameters. FTIR analysis showed that the hydroxyl, carboxyl, alcohol, and amide groups are the major groups that responsible for the biosorption process. The sorption isotherm is successfully modeled by the Temkin and Pyzhey model. Thermodynamic study revealed that there is an exothermic nature of the reaction between GG sites and RO dye molecules.

### Acknowledgments

We would like to express our sincere thanks to the Environmental Engineering Department, University of Baghdad, Iraq, for supporting this work.

## References

- [1] Ahmad, R. and Kumar, R., 2010, *Adsorption Studies of Hazardous Malachite Green onto Treated Ginger Waste*. J. Environ. Manage., Vol. (91), No. (4), PP. 1032-1038.
- [2] Al-Rub, A.A., El-Naas, M.H., Ashour, I., and Al-Marzouqi, M., 2006, *Biosorption of copper on Chlorella vulgaris from single, binary and ternary metal aqueous solutions, process*, Biochem., Vol. (41), PP. 457-464.
- [3] Anwar, J., Shafique, U., Waheeduz, Z., Salman, M., Dar, A. and Anwar, S., 2010, *Removal of Pb(II) and Cd(II) From Water by Adsorption on Peels of Banana*, J. Bioresource Technology, Vol.(101),PP. 1752–1755.
- [4] Arief, V.O., Trilestari, K., Sunarso, J., Indraswati, N., and Ismadji, S., 2008, *Recent Progress on Biosorption of Heavy Metals From Liquids using Low Cost Biosorbents: Characterization, Biosorption Parameters and Mechanism Studies*, a review, Clean., Vol. (36), PP. 937-962.
- [5] Bertagnolli, C., Da Silva, M., and Guibal, E., 2014, *Chromium Biosorption Using the Residue of Alginate Extraction from Sargassum Filipendula*, Chemical Engineering Journal, Vol. (237), PP. 362–371.
- [6] Bhatnagar A., and Jain, A.K., 2005, *A Comparative Adsorption Study with Different Industrial Wastes as Adsorbents for the Removal of Cationic Dyes from Water*, J. Colloid Interface Sci., Vol.(281), PP. 49-55.
- [7] Bhatti, H.N., and Safa, Y., 2012, *Removal of Anionic Dyes by Rice Milling Waste from Synthetic Effluents: Equilibrium and Thermodynamic Studies*, Desalination and Water Treatment, Vol. (48), PP. 267-277.
- [8] Bizani, E., Fytianos, K., Poullos, I., and Tsiroidis, V., 2006, *Photocatalytic Decolorization and Degradation of Dye Solutions and Wastewaters in the Presence of Titanium Dioxide*. J. hazard. Mater., Vol. (136), PP. 85-94.
- [9] Chojnacka, K., 2006, *Biosorption of Cr(III) Ions by Wheat Straw and Grass: a Systematic Characterization of New Biosorbents*, Polish J. Environ Stud., Vol. (15), PP. 845–52.
- [10] Chung, K.T., Fulk, G.E., and Andrews, A.W., 1981, *Mutagenicity Testing of Some Commonly Used Dyes*, Appl. Environ. Microbiol., Vol. (42), PP. 641-648.
- [11] Dada, A.O., Olalekan, A.P., Olatunya, A.M., and Dada O., 2012, *Langmuir, Freundlich, Temkin and Dubinin–Radushkevich Isotherms Studies of Equilibrium Sorption of Zn<sup>2+</sup> onto Phosphoric Acid Modified Rice Husk*, IOSR Journal of Applied Chemistry, Vol. (3), No. (1), PP. 38-45.
- [12] El-Sayed, G.O., Aly, H.M., and Hussien, S.H.M., 2011, *Removal of Acrylic Dye Blue-5G from Aqueous Solution by Adsorption on Activated Carbon Prepared from Maize Cops*, International Journal of Research in Chemistry and Environment, Vol. (1), No. (2), PP. 132-140.
- [13] Elwakeel, K.Z., Atia A.A., and Guibal E., 2014, *Fast Removal of Uranium from Aqueous Solutions using Tetraethylenepentamine Modified Magnetic Chitosan Resin*, Bioresour. Technol., <http://dx.doi.org/10.1016/j.biortech.2014.01.037>
- [14] Freundlich, H.M.F., 1906, *Over the Adsorption in Solution*, Journal of Physical Chemistry, Vol. (57), PP. 385-407.
- [15] Hameed, B.H., Mahmoud D.K., and Ahmed, A.L., 2008, *Sorption Equilibrium and Kinetics of Basic Dye from Aqueous Solution Using Banana Stalk Waste*, J. Hazar. Mater., Vol. (158), PP. 499-506.



- [16] Han, M.H., and Yun, Y.S., 2007, *Mechanistic Understanding and Performance Enhancement of Biosorption of Reactive Dyes by the Waste Biomass Generated from Amino Acid Fermentation Process*, *Biochem. Eng. J.*, Vol. (36), PP. 2-7.
- [17] Haq. J., Bhatti, H.N., and Asgher, M., 2011, *Removal of Solar Red BA Textile Dye from Aqueous Solution by Low Cost Barely Husk: Equilibrium, kinetic and thermodynamic study*, *The Canadian J. Chem. Eng.* Vol. (89), No (3), PP. 593-600.
- [18] Hossain M.A., Ngo H.H., Guo W.S., and Setiadi T., 2012, *Adsorption and Desorption of Copper(II) Ions Onto Garden Grass*, *J. Bioresource Tech.*, Vol.(121), PP. 386-395.
- [19] Jiang. Y., Sun. Y., Lui. H., Zhu. F., and Yin H., 2008, *Solar Photocatalytic Decolorization of C.I. Basic Blue 41 in an Aqueous Suspension of TiO<sub>2</sub>-ZnO*. *Dyes Pigm.*, Vol. (78), PP. 77-83.
- [20] Kookana, R.S., and Rogers, S.L., 1995, *Effects of Pulp Mill Effluent Disposal on Soil*, *Rev. Environ. Contam. Toxicol.*, Vol.(142), PP. 13-64.
- [21] Kratochvil, D., and Volesky, B., 1998, *Advances in Biosorption of Heavy Metals*, *J. Trend Biotechnol.*, Vol. (16), PP. 291–300.
- [22] Langmuir, I., 1918, *The Adsorption of Gases on Plane Surfaces of Glass, Mica and Platinum*. *J. Am. Chem. Soc.*, Vol. (40), No. (9), PP. 1361-1403.
- [23] Li C., Li W., and Wei L., 2012, *Research on Absorption of Ammonia by Nitric Acid-Modified Bamboo Charcoal at Low Temperature*, Vol. (47), PP. 3-10.
- [24] Liu Y., 2009, *Is the Free Energy Change of Adsorption Correctly Calculated?*, *J. Chem. Eng. Data*, Vol. (54), PP. 1981-1985.
- [25] Lodeiro, P., Cordero, B., Grille, Z., Herrero, R., and Vicente, M.E., 2004, *Physicochemical Studies of Cadmium (II) Biosorption by the Invasive Alga in Europe: Sargassum Muticum*, *Biotechnol. and Bioeng.*, Vol. (88), No. (2), PP. 237-247.
- [26] Mahmoud, A.S., Brooks, M.S., and Ghaly, A.E., 2007, *Decolonization of Remazol Brilliant Blue Dye Effluent by Advanced Photo Oxidation Process (H<sub>2</sub>O<sub>2</sub>/UV System)*. *Amer. J. App. Sci.*, Vol. (4), No. (12), PP. 1054-1063.
- [27] Mall, I.D., Srivastava, V.C., Agarwall, N.K., and Mishra I.M., 2007, *Removal of Congo Red on Coal Based Mesoporous Activated Carbon*, *Dye Pigments*, Vol. (74), PP. 34-40.
- [28] Meena, A.K, Mishra, G.K., Rai, P.K., Rajagopal. C., and Nagar, P.N., 2005, *Removal of Heavy Metal Ions from Aqueous Solutions using Carbon Aerogel as an Adsorbent*, *J. Hazard. Mat.*, Vol. (122), PP. 161–170.
- [29] Mittal, A., 2006, *Adsorption Kinetics of Removal of a Toxic Dye, Malachite Green, from Wastewater by using Hen Feathers*, *J. Hazard. Mater.*, Vol. (133), No. (1-3), PP. 196-202.
- [30] Mittal, A., Kaur, D., and Mittal, J., 2009, *Batch and Bulk Removal of Triarylmethane Dye, Fast Green FCF, from Wastewater by Adsorption over Waste Materials*. *J. Hazard. Mater.*, Vol. (163), PP. 568-577.
- [31] Moreira, R.F., Kuhen, N.C., and Peruch, M.G., 1998, *Adsorption of Reactive Dyes onto Granular Activated Carbon*, *Latin Am. Appl. Res.* Vol. (28), PP. 37–41.
- [32] Owoyokun, T.O., 2009, *Biosorption of Methylene Blue Dye Aqueous Solution on Delonix Regia (Flamboyant Tree) Pod Biosorbent*, *The Pacific Journal of Science and Technology*, Vol. (10), No. (2), PP. 872-883.
- [33] Pereira, L., Sousa, A., Coelho, H., Amado, A.M., and Ribeiro-Claro. P.J.A., 2003, *Use of FTIR, FT-Raman and 13C-NMR spectroscopy for identification of some seaweed phycocolloids*, *J. Biomol. Eng.*, Vol. (20), PP. 223–228.

- [34] Prasad, A.L., and Santhi, T., 2012, *Adsorption of Hazardous Cationic Dyes from Aqueous Solution onto Acacia Nilotica Leaves as an Ecofriendly Adsorbent*, Sustain. Environ. Res., Vol. (22), PP. 113-122.
- [35] Quintelas, C., Fernandes, B., Castro, J., Figueiredo, H., and Tavares, T. 2008, *Biosorption of Cr(VI) by three different bacterial species supported on granular activated carbon—a comparative study*, J. Hazard. Mater., Vol. (153), PP. 799–809.
- [36] Saleem, M., Pirzada, T., and Qadeer, R., 2007, *Sorption of Acid Violet 17 and Direct Red 80 Dyes on Cotton Fiber from Aqueous Solutions*, J. Colloids Surf., Vol. ( 292), PP. 246–250.
- [37] Sari, A., and Tuzen, M., 2008, *Biosorption of Cadmium (II) from Aqueous Solution by Red Algae (Ceranium Virgatum): Equilibrium, Kinetic and Thermodynamic Studies*. J. Hazard. Mat., Vol. (157), PP. 448–454.
- [38] Sharma, N., and Nandi, B.K., 2013, *Utilization of Sugarcane Baggase, an Agricultural Waste to Remove Malachite Green Dye from Aqueous Solutions*, J. Mater. Environ. Sci., Vol. (4), No. (6), PP. 1052-1065.
- [39] Sulaymon, A.H, Mohammed, A.A, and Al-Musawi, T.J., 2014, *Comparative Study of Removal of Cadmium (II) and Chromium (III) Ions from Aqueous Solution Using Low-Cost Biosorbent*, Int. J. Chem. Reac. Eng., Vol (12), No. (1), PP. 1-10.
- [40] Sulaymon, A.H., Mohammed, A.A., and Al-Musawi, T.J., 2013, *Removal of Lead, Cadmium, Copper, and Arsenic Ions using Biosorption: Equilibrium and Kinetic Studies*, Desalination and Water Treatment, Vol. (51), PP. 4424-4434.
- [41] Temkin, M.J., and Pyzhey, V., 1940, *Recent Modification to Langmuir Isotherm*, Acta. Physiochim., Vol. (12), PP. 217-222.
- [42] Thinakaran, N., Baskaralingam, P., Pulikesi, M., Panneerselvam, P., and Sivanesan, S., 2007, *Removal of Acid Violet 17 from Aqueous Solutions by Adsorption onto Activated Carbon Prepared from Sunflower Seed Hull*, J. Hazard. Mater., Vol.(151), PP. 316-312.

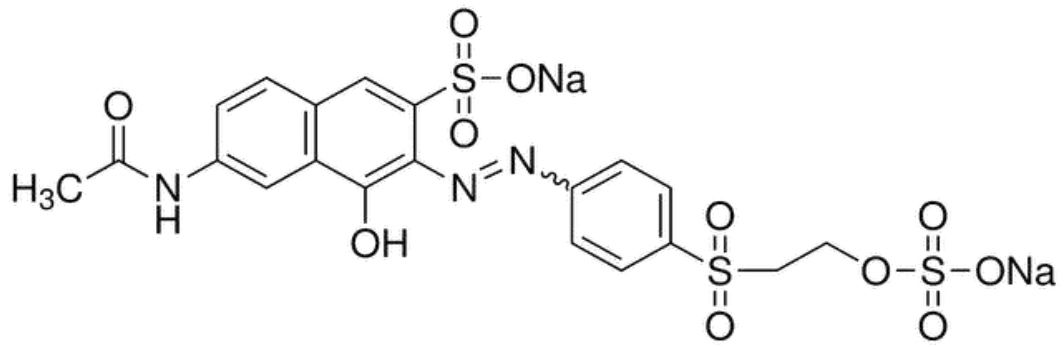


**Figure 1.** Chemical structure of RO dye, **Moreira, et al., 1998.**

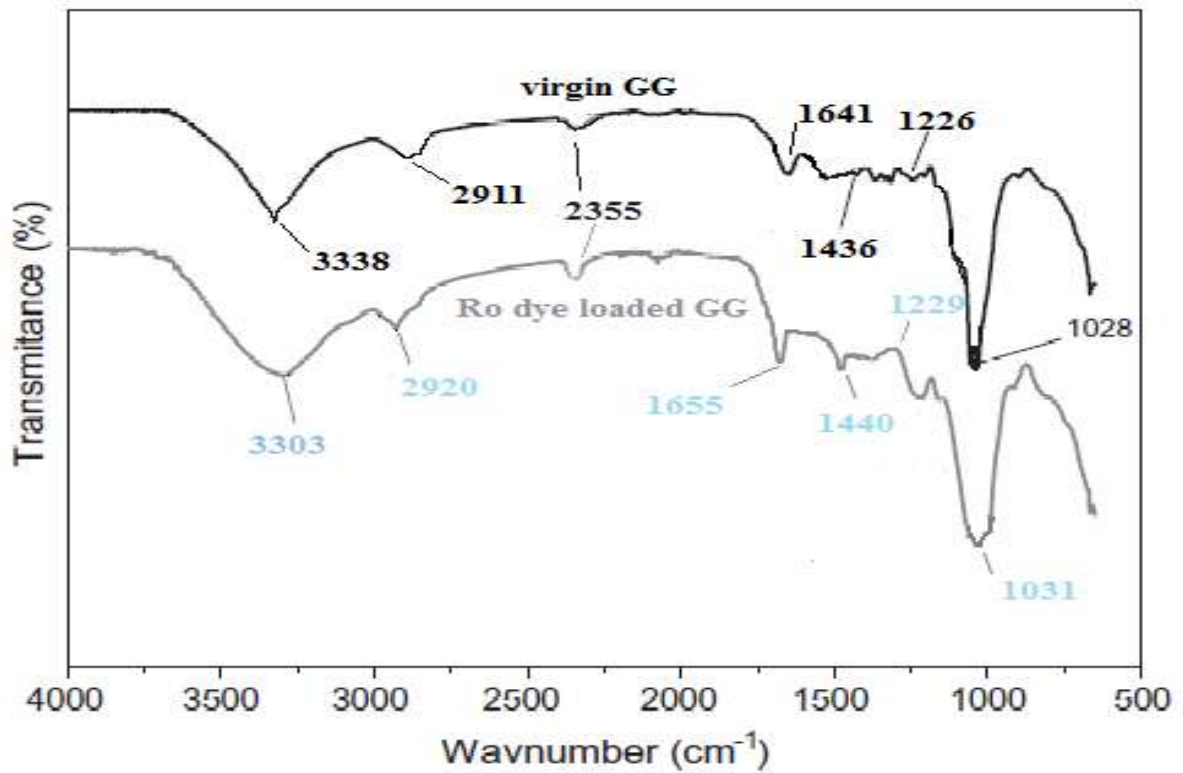


**Figure 2.** FTIR spectrum of virgin and RO loaded GG samples.

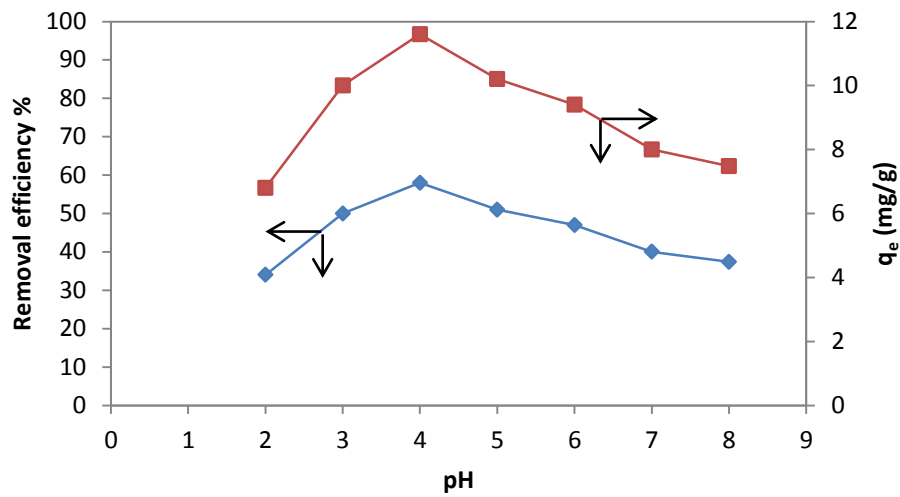


**Figure 3.** PH effect on RO dye sorption using GG ( $C_o=10$  mg/l, GG dose=1 g, room temperature, 2 h contact time at 200 rpm).

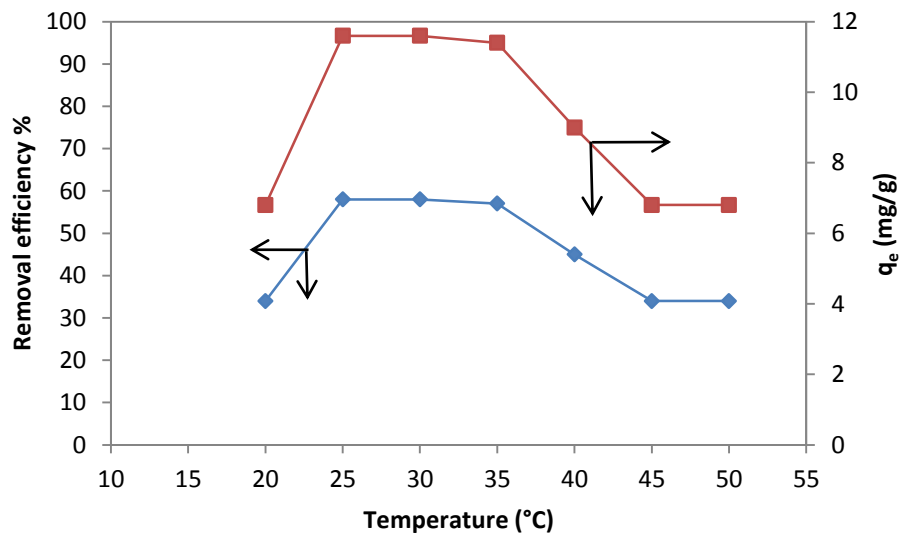


**Figure 4.** Temperature effect on RO dye sorption using GG ( $C_o=10$  ppm, GG dose=1 g, pH=4, 2 h contact time at 200 rpm).

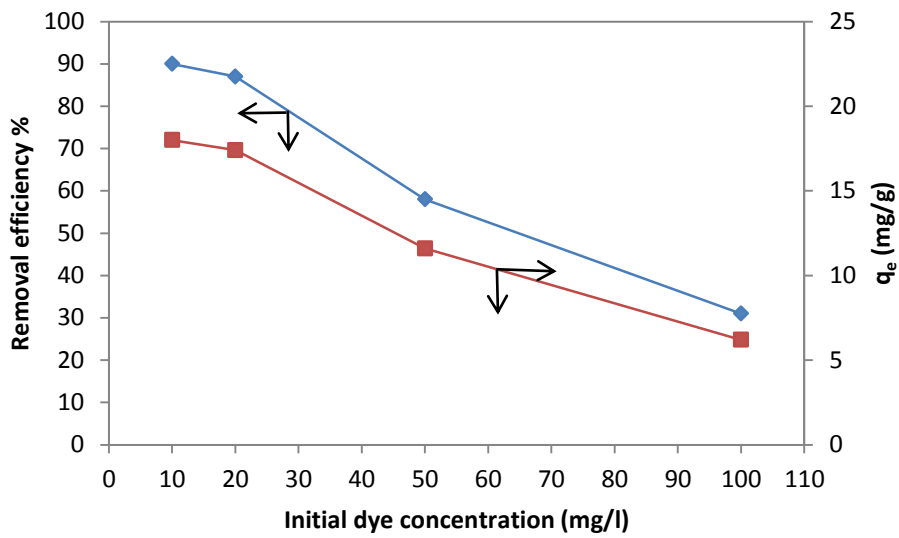


**Figure 5.** Initial RO dye concentration effect on the removal efficiency using GG: (GG dose=1 g, pH=4, room temperature, 2 h contact time at 200 rpm).

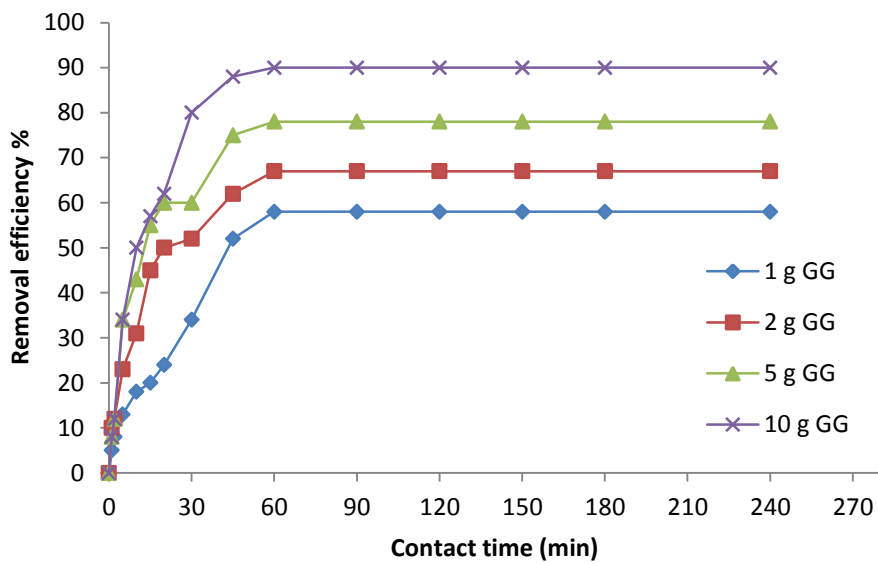


**Figure 6.** Effect of contact time on the removal efficiency of RO dye using different GG dosages: (pH=4, room temperature, at 200 rpm).

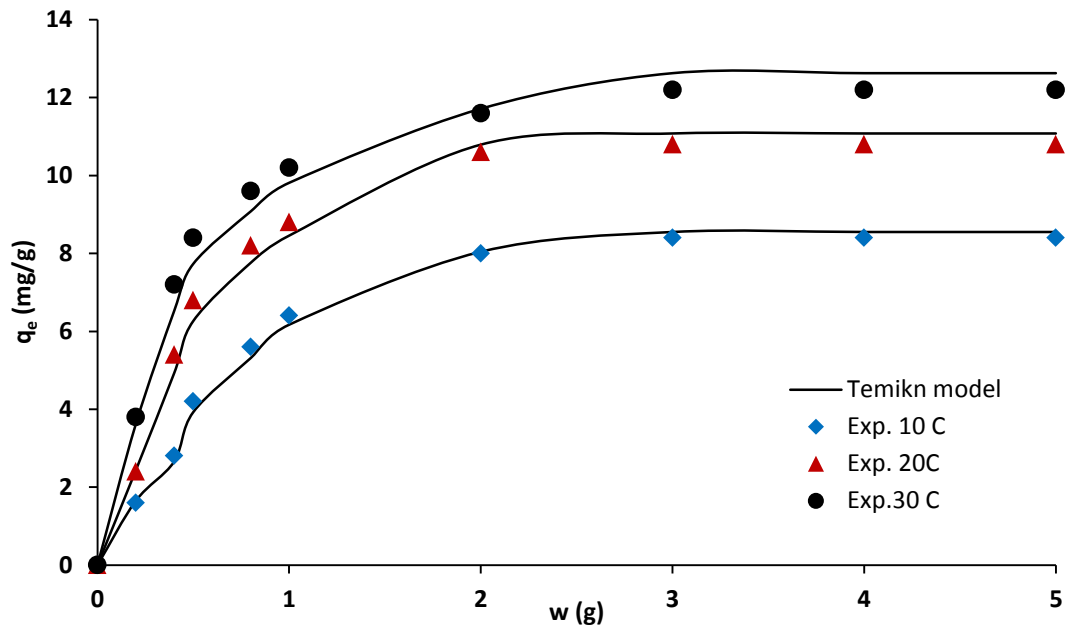


**Figure 7.** RO biosorption capacity using GG at different temperature:  $C_o=10$  mg/l, GG weight ( $w$ ) =0-5 g, pH=4, contact time= 2h, at 200 rpm.

**Table1.** The equations for the sorption isotherm.

| Model             | Equation   | Reference                       | No. |
|-------------------|--|---------------------------------|-----|
| Langmuir          | $q_e = \frac{q_m K_L C_e}{1 + K_L C_e}$  | <b>Langmuir, 1918</b>           | (3) |
|                   | q <sub>e</sub> is the sorption uptake (mg/g); C <sub>e</sub> is the equilibrium concentration of the adsorbate (mg/l); q <sub>m</sub> is the maximum amount of the adsorbate per unit weight of the adsorbent (mg/g); K <sub>L</sub> is the Langmuir constant related to the free energy of sorption (l/mg). |                                 |     |
| Freundlich        | $q_e = K_F C_e^{1/n}$  | <b>Freundlich, 1906</b>         | (4) |
|                   | q <sub>e</sub> is the sorption uptake (mg/g); C <sub>e</sub> is the equilibrium concentration of the adsorbate (mg/l); n is the Freundlich constant related to sorption intensity (g/l); K <sub>F</sub> is the Freundlich constant related to the relative sorption capacity (mg/g).                         |                                 |     |
| Temkin and Pyzhey | $q_e = \frac{RT}{b_{T_e}} \ln(a_{T_e} C_e)$  | <b>Temkin, and Pyzhey, 1940</b> | (5) |
|                   | T is the absolute temperature (K), R is the universal gas constant (8.314 J/mol. K), a <sub>T<sub>e</sub></sub> is the equilibrium binding constant, b <sub>T<sub>e</sub></sub> is corresponding to the heat of sorption, and C <sub>e</sub> is the equilibrium concentration of the adsorbate (mg/l).       |                                 |     |
| Redlich-Peterson  | $q_e = \frac{k_{RP} C_e}{1 + \alpha_{RP} C_e^{\beta_{RP}}}$  | <b>Quintelas, et al., 2008</b>  | (6) |
|                   | q <sub>e</sub> is the sorption uptake (mg/g); C <sub>e</sub> is the equilibrium concentration of the adsorbate (mg/l); k <sub>RP</sub> , α <sub>RP</sub> and β <sub>RP</sub> are constants.  |                                 |     |
| Van't Hoff        | $\ln K_c = -\frac{\Delta H^\circ}{RT} + \frac{\Delta S^\circ}{R}$  | <b>Liu, 2009</b>                | (7) |
|                   | K <sub>c</sub> is the equilibrium constant (q <sub>e</sub> /C <sub>e</sub> ), R is the universal gas constant (8.314 J/mol. K), ΔH° is the enthalpy of the sorption (kJ/mol), ΔS° is the entropy of the sorption (J/K.mol), and T is the solution temperature (K).   |                                 |     |
| Gibbs free energy | $\Delta G^\circ = -RT \ln K_c$   | <b>Liu, 2009</b>                | (8) |
|                   | ΔG° is the Gibbs free energy of biosorption (kJ/mol), K <sub>c</sub> is the equilibrium constant (q <sub>e</sub> /C <sub>e</sub> ), R is the universal gas constant (8.314 J/mol. K), and T is the solution temperature (K).   |                                 |     |

**Table 2.** Characterization of the powdered grass.

| Parameter                              | Value |
|--|-------|
| Particle size (mm)                     | <0.2  |
| Surface area (m <sup>2</sup> /g)       | 5.6   |
| Apparent density (g/l)                 | 0.48  |
| Zero point charge (pH <sub>zpc</sub> ) | 5.1   |
| Porosity (%)                           | 60.5  |
| Moisture content (%)                   | 1.57  |
| Ash content (%)                        | 0.99  |

**Table 3.** Parameters of isotherm models for the biosorption of RO dye onto GG.

| Model             | Equation  | Parameters   | At 10 °C                          | At 20 °C                          | At 30 °C                          |
|-------------------|---|--|-----------------------------------|-----------------------------------|-----------------------------------|
| Langmuir          | $q_e = \frac{q_m K_L C_e}{1 + K_L C_e}$                     | $q_m$ , mg/g<br>$K_L$ , l/mg<br>$R^2$                              | 0.857<br>-0.018<br>0.813          | 1.554<br>-0.023<br>0.826          | 2.616<br>-0.029<br>0.884          |
| Freundlich        | $q_e = K_F C_e^{1/n}$                                       | $K_f$ , mg/g<br>$n$ , g/l<br>$R^2$                                 | 14.849<br>-0.321<br>0.925         | 10.079<br>-0.503<br>0.903         | 7.732<br>-0.709<br>0.917          |
| Temkin and Pyzhey | $q_e = \frac{RT}{b_{Te}} \ln(a_{Te} C_e)$                   | $B = RT/b_{Te}$ , l/mg<br>$a_{Te}$ , mg/g<br>$R^2$                 | 14.962<br>102.713<br>0.995        | 13.332<br>105.603<br>0.988        | 12.330<br>108.630<br>0.980        |
| Ridlich-Peterson  | $q_e = \frac{k_{RP} C_e}{1 + \alpha_{RP} C_e^{\beta_{RP}}}$ | $k_{RP}$ , mg/g<br>$\alpha_{RP}$ , l/mg<br>$\beta_{RP}$ ,<br>$R^2$ | 22.040<br>0.991<br>0.567<br>0.891 | 12.553<br>1.133<br>1.041<br>0.789 | 30.339<br>1.008<br>0.889<br>0.782 |

**Table 4.** Uptake of organic materials by different biomasses.

| Material            | Biomass                | $q_e$ (mg/g) | Reference               |
|---------------------|------------------------|--------------|-------------------------|
| Crystal Violet dye  | Acacia nilotica leaves | 33           | Prasad and Santhi, 2012 |
| Rhodamine B dye     | Acacia nilotica leaves | 37           | Prasad and Santhi, 2012 |
| Malachite green dye | Hen feather            | 26           | Mittal, 2006            |
| Malachite Green Dye | Sugarcane baggase      | 22           | Sharma and Nandil, 2013 |
| Reactive orange dye | Garden grass           | 12.7         | This study              |

**Table 5.** Thermodynamic constants of biosorption of RO dye onto GG.

| Temperature (K) | $\Delta G^\circ$ (kJ/mol) | $\Delta H^\circ$ (kJ/mol) | $\Delta S^\circ$ (J/mol.K) | $R^2$ |
|-----------------|---------------------------|---------------------------|----------------------------|-------|
| 293             | 1.282                     | -43.521                   | -0.152                     | 0.912 |
| 298             | 3.188                     |                           |                            |       |
| 303             | 3.241                     |                           |                            |       |
| 308             | 3.400                     |                           |                            |       |
| 313             | 4.710                     |                           |                            |       |
| 318             | 6.090                     |                           |                            |       |
| 323             | 6.103                     |                           |                            |       |